

# FDG-PET Appearance of Pelvic Castleman's Disease

Stephen P. Murphy, Mark A. Nathan and Mark W. Karwal

Departments of Radiology and Internal Medicine, The University of Iowa College of Medicine, Iowa City, Iowa

We report a case of Castleman's disease demonstrating  $^{18}\text{F}$ -fluorodeoxyglucose (FDG) localization by whole-body PET imaging in a pelvic soft-tissue mass shown on abdominopelvic CT. In this case, there is mild FDG localization within pelvic Castleman's disease with standard uptake values lower than in many cases of low-grade and intermediate-grade lymphomas previously reported. FDG-PET may be of value as an imaging modality for differentiating Castleman's disease from lymphoma.

**Key Words:** Castleman's disease; fluorine-18-FDG; PET

**J Nucl Med 1997; 38:1211-1212**

Castleman's disease is a rare benign lymphoproliferative disorder first described in 1954 in a patient with a large mediastinal mass (1,2). Approximately 70% of lesions occur within the thorax; however, masses may be seen in any region of the body where lymphoid tissue is normally present (3). Castleman's disease may be divided into two histologic types: the hyaline-vascular type, which accounts for more than 90% of the cases and the less common plasma-cell type (4). A multicentric form of Castleman's disease, most often the plasma-cell type, has been reported and is characterized by constitutional symptoms, multicentric lymphadenopathy and hepatosplenomegaly (5-8). Multicentric Castleman's disease may degenerate into lymphoma or Kaposi's sarcoma and thus lead to significant morbidity and mortality (8). In this report, we present a case of pelvic Castleman's disease imaged with  $^{18}\text{F}$ -FDG PET.

## CASE REPORT

A 31-yr-old woman presented with a 3 mo history of left lower quadrant abdominal pain accompanied by poor appetite and a 5-kg weight loss. An abdominopelvic CT scan performed elsewhere earlier revealed a low-attenuation pelvic mass thought to represent an ovarian cyst. An exploratory laparotomy showed a 7-cm retroperitoneal soft-tissue mass. Needle biopsy obtained reactive lymphoid tissue but was nondiagnostic.

A subsequent contrast-enhanced abdominopelvic helical CT revealed a left hemipelvic soft-tissue mass containing punctate calcifications (Fig. 1). Additional soft-tissue adenopathy was seen along the right iliac vessels. The small low-attenuation fluid collection along the anteromedial aspect of the left hemipelvic mass was thought to represent a small resolving hematoma from the biopsy performed.

In fasting state (serum glucose 54 mg/dl), the patient received 9.6 mCi (355 MBq) of FDG intravenously. A whole-body PET study was performed with image acquisition starting at 40 min after FDG injection. Emission data was acquired for nine consecutive bed positions (10-cm field of view). The bladder was flushed with normal saline via foley during the examination to remove bladder activity. A  $^{68}\text{Ge}/^{68}\text{Ga}$  pin-source transmission study was obtained after the emission study. Non- and attenuation corrected whole-

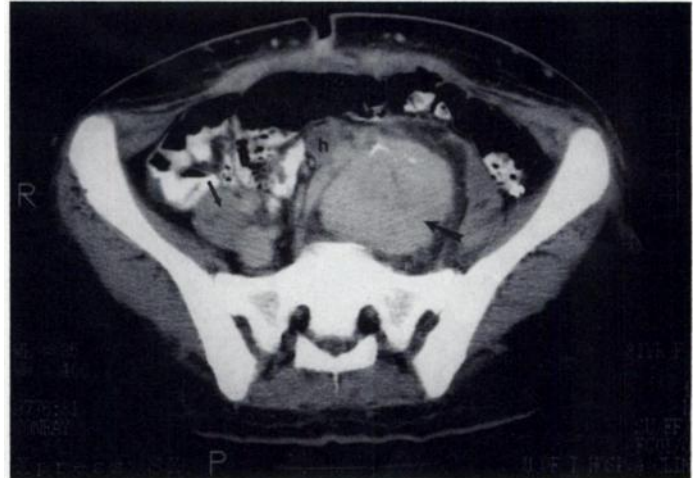


**FIGURE 1.** Contrast-enhanced CT image through the pelvis demonstrates a large homogeneously enhancing mass (6 × 7 × 7 cm) with a few punctate calcifications in the left hemipelvis (large arrow). Associated right iliac lymphadenopathy measuring 3 × 2.5 × 3 cm (small arrow) and a small resolving postbiopsy hematoma (h) can also be seen.

body images were then reconstructed by filtered backprojection combining the data from the consecutive 10-cm fields of view.

The patient's FDG-PET images showed a focus of radiotracer accumulation in the pelvic soft-tissue mass as well as the enlarged right iliac nodes (Fig. 2). Standard uptake values (SUVs) for the pelvic mass and the right iliac nodes ranged from 2.3-3.2 and from 1.8-2.7, respectively.

A second surgical biopsy was performed after CT and PET imaging. The mass was noted at surgery to be richly hypervascular. The pathologic diagnosis was Castleman's disease, hyaline-vascular type.

## DISCUSSION

The radiologic appearance of Castleman's disease is nonspecific; the differential diagnosis includes granulomatous disorders, inflammatory lymphadenopathy and malignant lesions such as lymphoma and metastatic tumor (9). As a consequence, the diagnosis is made by biopsy or surgical resection. Thus, an imaging modality that helps to differentiate the benign lymphoproliferative changes of Castleman's disease from malignant lymphoma might reduce the inherent morbidity of biopsy and surgical management (10).

FDG accumulation in the pelvic mass in this patient was modest with SUVs of 2.3-3.2. The regional disease in the contralateral right iliac lymph nodes had slightly lower SUVs of 1.8-2.7. There are two possible explanations for these lower SUVs relative to the primary left hemipelvic mass: The right iliac adenopathy, although not biopsied, may have been less extensively involved by lymphoproliferative changes than the left-sided mass. Keller et al. (4) report that in 44 of 74 hyaline-vascular type lesions, areas of remnant normal lymph node could be identified. Right iliac focus of activity and the corresponding regions of interest drawn in this area were quite small and, therefore, the SUVs may have been lowered by partial volume effects.

Received May 13, 1996; revision accepted Nov. 23, 1996.  
For correspondence or reprints contact: Mark A. Nathan, MD, Department of Radiology, The University of Iowa Hospitals and Clinics, 200 Hawkins Dr., Iowa City, IO 52242.

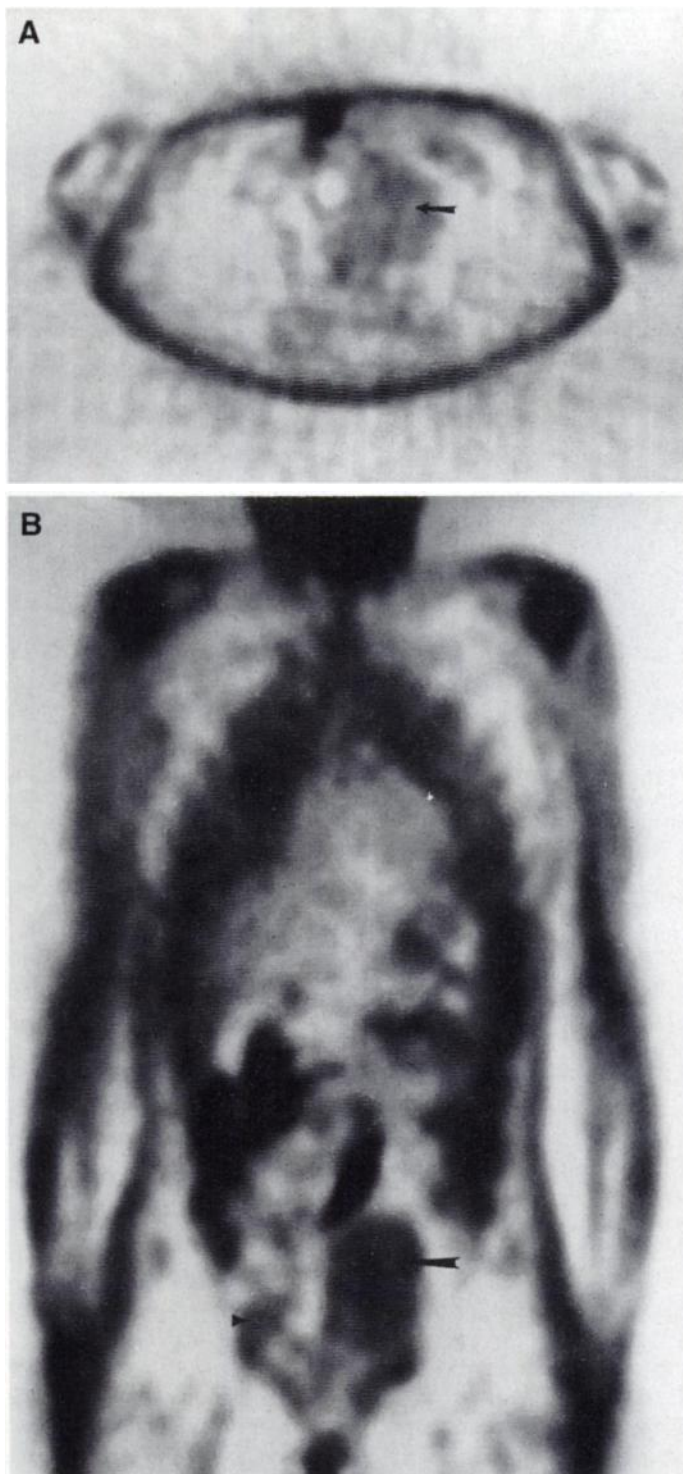


**FIGURE 2.** (A) Nonattenuation corrected transaxial and (B) coronal FDG-PET images show an area of abnormal radiotracer localization (arrow) corresponding to the left hemipelvic soft-tissue mass seen on CT. An additional smaller focus of abnormal activity (arrowhead) is seen in the region of the right iliac adenopathy. Note the abdominal foci of increased tracer localization corresponding to the ascending colon/right kidney (right), the surgical biopsy incision (midline above the pelvic soft-tissue mass) and the descending colon (left).

Previous PET studies have shown mild FDG localization in low- and some intermediate-grade lymphomas. Leskinen-Kallio et al. (11) reported SUVs of 1.9–11.0 in nine patients who showed FDG accumulation in low- and intermediate-grade lymphomas with seven of these patients having SUVs greater than 3.2. Newman et al. (12) reported SUVs in 10 patients with low- and intermediate-grade lymphomas in a range of 2.4–18.7 with most being higher than the maximum SUV of 3.2 in this patient. In our limited experience, four patients with FDG localization in low- and intermediate-grade lymphomas showed SUVs of 3.3–23.4.

Studies of  $^{67}\text{Ga}$  SPECT in the evaluation of Castleman's disease have been limited (9,13). Burke et al. (13) first reported  $^{67}\text{Ga}$  localization in Castleman's disease presenting as a retroperitoneal mass in an adolescent with anemia. Subsequently, one group reported that  $^{67}\text{Ga}$  accumulated in Castleman's disease to a lesser degree than that seen with lymphoma (9). This would suggest  $^{67}\text{Ga}$  SPECT as a possible imaging modality to help differentiate Castleman's disease from lymphoma, but due to the small number of patients evaluated with SPECT to date, further studies may be necessary to confirm this observation.

## CONCLUSION

PET imaging of Castleman's disease demonstrated FDG accumulation in a range lower than that seen in four patients with low- and intermediate-grade lymphomas at our institution and lower than that seen for most low- and intermediate-grade lymphomas previously reported (11,12). These findings suggest the use of FDG-PET as an imaging modality to differentiate benign Castleman's disease from malignant lymphoma.

## REFERENCES

1. Castleman B, Towne VW. Case records of the Massachusetts General Hospital: case 40011. *N Engl J Med* 1954;250:26–30.
2. Castleman B, Iverson L, Menendez VP. Localized mediastinal lymph node hyperplasia resembling thymoma. *Cancer* 1956;9:822–830.
3. Goldberg MA, DeLuca SA. Castleman's disease. *Am Fam Physician* 1989;40:151–153.
4. Keller AR, Hochholzer L, Castleman B. Hyaline-vascular and plasma-cell types of giant lymph node hyperplasia of the mediastinum and other locations. *Cancer* 1972;29:670–683.
5. Gaba AR, Stein RS, Sweet DL, Variakojis D. Multicentric giant lymph node hyperplasia. *Am J Clin Pathol* 1978;69:86–90.
6. Frizzera G, Banks PM, Massarelli G, Rosai J. A systemic lymphoproliferative disorder with morphologic features of Castleman's disease. Pathological findings in 15 patients. *Am J Surg Pathol* 1983;7:211–231.
7. Weisenburger DD, Nathwani BN, Winberg CD, Rappaport H. Multicentric angiofollicular lymph node hyperplasia: a clinicopathologic study of 16 cases. *Hum Pathol* 1985;16:162–172.
8. Lisbon E, Fields S, Strauss S, et al. Widespread Castleman's disease: CT and US findings. *Radiology* 1988;166:753–755.
9. Yamashita Y, Hirai T, Matsukawa T, Ogata I, Takahashi M. Radiological presentations of Castleman's disease. *Comput Med Imaging Graph* 1993;17:107–117.
10. Griffith LK, Dehdashti F, McGuire AH, et al. PET evaluation of soft-tissue masses with fluorine-18-fluoro-2-deoxy-D-glucose. *Radiology* 1992;182:185–194.
11. Leskinen-Kallio S, Ruotsalainen U, Nagren K, Teras M, Joensuu H. Uptake of carbon-11-methionine and fluorodeoxyglucose in non-Hodgkin's lymphoma: a PET study. *J Nucl Med* 1991;32:1211–1218.
12. Newman JS, Francis IR, Kaminski MS, Wahl RL. Imaging of lymphoma with PET with  $2[^{18}\text{F}]$ fluoro-2-deoxy-D-glucose: correlation with CT. *Radiology* 1994;190:111–116.
13. Burke GJ, Wei J. Retroperitoneal mass and anemia in an adolescent. *Invest Radiol* 1992;27:748–750.